Team Name: Virginia Tech Mapping Autonomous Ground Vehicle (VT-MAGV)

Date: 05/09/2011

Advisors: Dr. Andrew Kurdila

Dr. Alexander Leonessa

Members: Tim Battis

Zhaoda (Adam) Deng

Yamilette Hernandez

Kyle Laaker

Jacob Lambeth

Braden O’Meara

Matt Pyrak

Fulton Smith

Introduction

The VT-MAGV team competing this year focused primarily on the design of a robust mechanical platform to be used initially for an autonomous 3D mapping and compressive sensing project. While IGVC was not our main focus, we were able to incorporate several of the design requirements into our platform design process so as to retain maximum flexibility for other projects in the future. Because of this, our own software development efforts have been limited, and the software architecture that will be used for IGVC is adapted from a sister project focused on designing an autonomous surface vehicle. In upcoming years, we expect future design teams at Virginia Tech to build upon our mechanical design and center their efforts on developing novel mapping and navigation strategies specifically for the IGVC competition. To this end, the following paper focuses on the design of a mechanical platform and does not attempt to describe the software architecture that will be implemented.

Mechanical Design:

The VT-MAGV vehicle was designed to meet specific operational criteria, namely, to: carry a large payload, reach speeds in excess of 10 mph, have an 8 hr endurance under normal operation, have zero turn radius, and be affordable enough to duplicate the design. In beginning the design process, the VT-MAGV team performed an extensive market survey to determine what types of commercial platforms are available off the shelf for use in autonomous applications. After extensive research, the team identified the Clearpath Robotics 'Husky A100', the ReflexRobotics 'Archer E' and the 21st Century Scientific 'Bounder' platforms as potential designs around which the MAGV could be modeled. These three designs and their stated specifications can be seen below in Table 1. The Bounder is an electric wheelchair after which our final design was modeled. Particularly attractive, the utilization of differential steering with castors allows for reliable telemetry while maintaining the low turn radius as well as a simple differential control scheme.

Table 1. Comparison of the three final commercial platforms selected as possible platform options. The comparison shows the best option, based on measurable specifications, is the Bounder platform.

Design Requirement:	**Husky A100**	**Archer E**	**Bounder**
Payload: 40 kg	45 kg	90 kg	100+ kg
Speed: 10 mph	3 mph	20 mph	11.6 mph
Zero turning radius	Yes (differential skid)	No (low radius)	Yes (differential + caster)
Endurance: 8 hr	2 hr	8 hr	8+ hr

Affordability	$13,000	$17,000	$12,000

In order to meet footprint requirements for the IGVC competition, a 36” length was selected, as measured from front to rear axles. Because it was felt that the robot should be able to pass through standard interior door frames, a width of 30” as measured from the limits of the drive tires was also selected as optimal. Pneumatic tires with a 13” inflated height have been selected for the design. The flexible sidewalls provide a limited suspension for the vehicle, while the large diameter relative to the height of obstacles and terrain that must be traversed results in a large mechanical advantage, reducing the amount of power required to travel across low bumps and curbs. Ground clearance was another area of concern for the design of the frame. The position of the motor mounting points and selection of 13” tall tires result in a 4” ground clearance. This should prove to be more than adequate for all movement profiles and required terrain types. The design process has incorporated a detail CAD model that has been iteratively updated in accordance with the needs of the design and the drivetrain team. An isometric 3-D model can be observed in Figure 1.

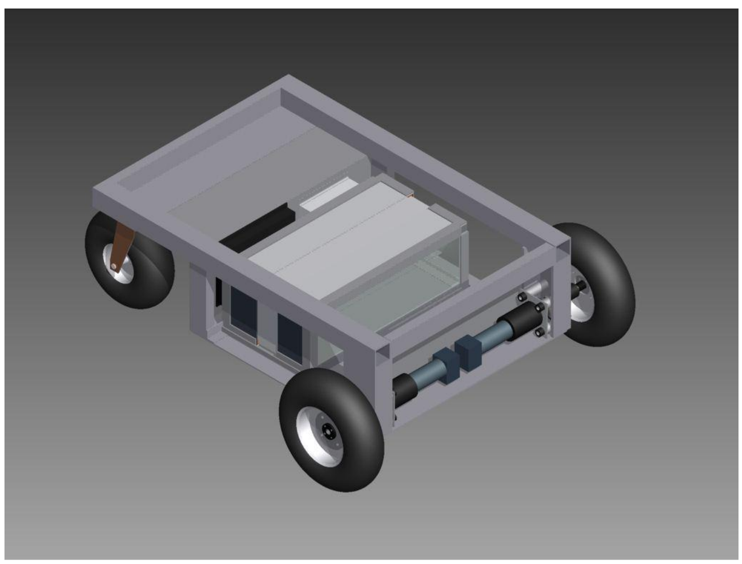

Figure 1. Isometric CAD model of the vehicle’s mechanical design

Based on the CAD models developed for the frame, the design team performed a basic finite element analysis on the frame structure using the integrated finite element analysis software in Autodesk Inventor. The constraints as defined by the design are the four wheel locations. Therefore, the frame was constrained in the vertical direction at the four wheel mount locations: two casters near the rear of the frame and two drive wheels at the front of the frame. Next, the team identified the dominant static loads. In the case of the robot design, the primary mass of the vehicle is due to the batteries. Therefore, the dominant load was represented as a pressure load evenly distributing the weight of the batteries in their installed location. See Figure 2 below for a screenshot of the meshed frame with the applied pressure load.

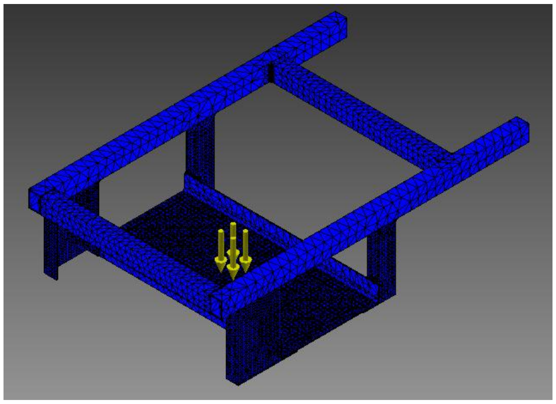

Figure 2. The image shows the constraints and loads applied to the frame for the finite element analysis. The constraints model the four wheels that limit vertical displacement. The load represents the weight of the batteries, the dominant force expected for static loading.

After applying the constraints and loads, the software was configured to ensure proper mesh density and stress convergence. In particular, the program was set to converge the Von Mises stresses to within 2%. The resulting mesh contained about 128,000 elements with a convergence of less than 1.1%. See Figure 3 below for the convergence plot. According to the results of the finite element analysis, the static stresses experienced by the frame are minimal compared to the yield strengths of commonly available metals like steel and aluminum. Additionally, the maximum stress is concentrated in a small, localized area. This means the worst case scenario is localized yielding, but complete failure is highly unlikely under normal operation.

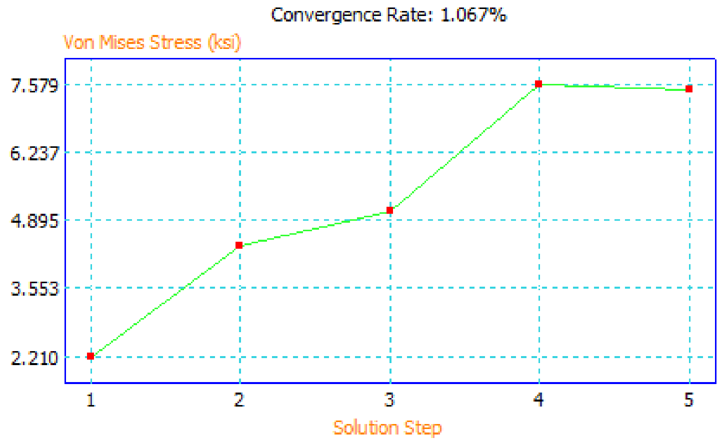

Figure 3. Convergence plot for the finite element analysis of the frame. The software successfully converged the Von Mises stresses to within 1.1% with a mesh of 128,000 elements.

Material Selection. The design team performed a trade-off analysis for readily available materials that had a 1/8 inch wall thickness and a 7.5 ksi maximum stress. In particular, a decision matrix analysis was performed on 1008 Steel, 4130 Steel, 6061 Aluminum and 6063 Aluminum components from McMaster-Carr. Table 2 shows the comparison chart used in the decision process. The effective stress concentration is an analytical number that was created using 7.5 ksi maximum stress seen in the FEA analysis. This max stress was scaled up if the evaluated material's wall thickness was less than 1/8 inch. Thus, the increased stress concentration was used to develop comparative safety factors for the four materials.

Table 2. Comparison table for the four selected material choices.

Material	**4130 Steel**	**1008 Steel**	**6061 Al**	**6063 Al**
Stress Concentration (psi) (based on 0.125" wall, 1"x2")	7500	7500	7500	7500
Wall thickness (in)	0.065	0.12	0.125	0.125
Effective stress concentration (psi)	14423.07	7812.5	7500	7500
Yield Strength (psi)	75000	41335.7	35000	16000
Factor of Safety	5.2	5.29097	4.66666	2.13333
Volume (in3)	97.4272	179.865	187.36	187.36
Density (lb/in3)	0.289018	0.28432	0.09754	0.09754
Weight	28.15824	51.1397	18.2757	18.2757
Price per foot ($/ft)	18.45	5.89	6.20	5.43
Total length	15	18	15	15
Total cost	276.7	106.08	92.95	81.5

The three parameters that the team focused on during the decision process were the factor of safety, weight, and cost. These parameters were assigned normalized scores based on the material that had the most desirable value for each category. For example, the material with the highest factor of safety was 1008 Steel, which was assigned a score of "1". Then, the other three materials received a normalized score on their safety factor relative to the 1008 Steel safety factor. Once the normalized scores were set, each parameter based was given a weighted score out of 100 based on its importance to the design. The factor of safety was considered to be the most important, and was given a weighted score of 50. The material weight was given a weighted score of 40, and the material cost was given a weighted score of 10. Table 3 displays the normalized scores, parameter weights, weighted scores and final scores for the four materials. The 6061 Aluminum finished with the highest score of 92.9, and was agreed upon by the design team as the best material choice.

The mechanical platform was made with 6061 high strength aluminum. The platform was built of ¼ inch box tubing, 1/8 inch sheet metal, as well as four pneumatic tires, two mounted on ball-bearing casters. The two drive wheels are mounted with bearings ordered from McMaster-Carr through their online division. In house tools were used to cut the box tubing to the correct dimensions, and then these pieces were brought to a local machine shop along with the full CAD drawings to be welded to our specifications. The team felt that it would be better to contract out the welding due to the team's lack of welding experience with the aluminum.

Table 3. Final scores for the four selected materials. Normalized scores were multiplied by the respective parameter weights and added together to give each material's final score.

Normalized scores (0 to 1)					
Material		**4130 Steel**	**1008 Steel**	**6061 Al**	**6063 Al**
Factor of safety		0.982805	1	0.882005	0.403202
Weight		0.649038	0.3573	1	1
Cost		0.294542	0.7682	0.87681	1
Weighted Scores					
Material	**Weight (%)**	**4130 Steel**	**1008 Steel**	**6061 Al**	**6063 Al**
Factor of safety	50	49.14026	50	44.1002	20.1601
Weight	40	25.96153	14.294	40	40
Cost	10	2.945428	7.6828	8.76815	10
Total		78.04723	71.977	92.8683	70.1601

Drivetrain Design:

The drivetrain design team pursued batteries, motors and gearboxes to provide the necessary propulsion capabilities as defined in the customer needs. The goal was to select drivetrain components capable of integrating into the final product to provide power and drive capabilities to propel the full mass of the vehicle with a minimum speed of 10 mph on varied terrain. Additionally, the motors were selected to provide the capability of climbing curbs and small obstacles.

Battery selection. After a thorough research on popular battery products on the market, the team found that there were three options in terms of battery types: lead acid, lithium polymer and lithium iron phosphate. Lead Acid battery is traditionally used in vehicles and they have very good performance. Lithium Iron phosphate (LIP) and lithium polymer (Li-Po) batteries are very similar in characteristics as they are both light and highly energy concentrated, however they require constant monitoring as well as cell balancing to achieve its maximum performance.

Based on the vehicle spec, it was found that in order to drive at 10mph on flat concrete surface; the battery has to provide a 30W power output for each motor. On flat grass surface, the power output requirement for each motor is approximately 150W. Taking into account the effect of inclination, a dynamic scenario was created in which during an 8 hour span, there is 1 hour sitting still, 1 hour running 5 degrees uphill on grass at 10mph, 1 hour running at 5 degree uphill on concrete at 10 mph, 2 hours running on flat grass surface at 10mph and 3 hours running on flat concrete surface at 10mph. The total approximate energy required for this dynamic scenario is 1600Wh. It is to be noted that the energy requirement is actually a lot higher for Lead Acid because it would add at least 30% more weight to the system for the same capacity. As far as Li-Po and LIP are concerned, this necessitates a 2000Wh battery because only 80-90% of the rated capacity can be used before it drops below the terminal cell voltage.

However, since factors such as the transmission resistance were not considered in the calculation, good practice requires an over-design to compensate for the lack of reliability in the estimation. Therefore, a 24V 100Ah battery pack is needed for the vehicle. Between LIP and Li-Po, they present similar traits but Lithium Polymer batteries have overheating issues when wet. On the other side, since a heavier vehicle would greatly reduce our maneuverability, we decided a lithium iron phosphate battery is more preferable than a heavier lead acid battery.

Battery Monitoring.

Together with the battery pack, an energy management system was also purchased that allows the computer to monitor the battery cell voltages, current drain, temperature and state of charge estimation. A central control module transmits battery information through a data collection module that is connected to the battery, and then communicates with the on-board computer. On the other hand, user can reconfigure the setting of charging and discharging limit on computer. A Labview VI was programmed with the MODBUS-RTU protocol to execute the serial communication.

Motor and gearbox selection.

The drivetrain design of the vehicle consists of an assembly that includes a motor, gearbox, and controller. A pair of brushless electric motors is used to drive the vehicle. Gearboxes are used to increase the torque provided by the motors. A controller is used to adjust the current provided to the motor and thus the speed it turns.

The vehicle’s performance goals influenced the design and ultimate choice for the motor. Our goal was for the vehicle to be able to travel at 10 mph on concrete. To travel at 10 mph, the vehicle requires a certain amount of power that is provided by the motors. Using simple torque and power calculations, along with force and moment balances, a proper motor was determined. Figure 4 shows a free body diagram of one wheel on the vehicle.

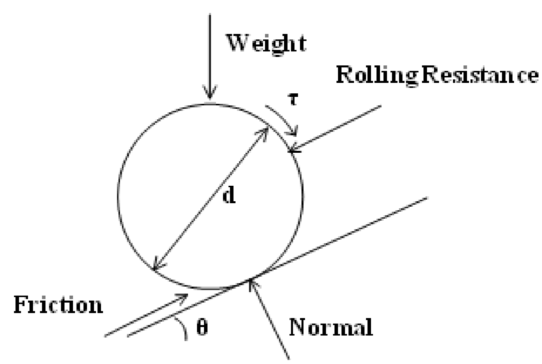

Figure 4. Free body diagram of vehicle tire on an incline

Rolling resistance is a resistive force caused by the deformation of a round object rolling on a surface. Rolling resistance, R, can be found from Equation 1:

$$R = C_{rr} * N \tag{1}$$

Where C_{rr} is the coefficient of rolling resistance and N is the normal force. C_{rr} has been found experimentally for a variety of cases. For a vehicle with pneumatic tires on concrete, it is estimated to be 0.017. Calculations were first performed assuming a slope of 0 degrees. Summing the forces on the tire and setting the acceleration to zero, the torque required to sustain a constant velocity was found.

$$\tau = C_{rr} * N * \frac{d}{2} \tag{2}$$

Using a C_{rr} of 0.017, a normal force of 333 N per tire, and a tire diameter of 13 inches, the estimated torque required is 0.936 N-m. Using torque power relationships, the required power for each motor to operate the vehicle at 10 mph is 25.3 W. Next, design team looked at a scenario of traveling up an inclined plane. The goal was to meet the performance specifications in an extreme scenario.

A similar approach of summing forces was taken to find the necessary torque needed to travel up a five degree concrete incline. The necessary torque to do this is 5.73 N-m. The angular velocity needed for this scenario is the same as on flat ground. The power required, however, is 155 W per motor.

Choosing the specific motor to be used was based on the price, lead time, voltage (24 V is preferable due to safety), maximum incline and maximum speed on flat concrete. It was determined to purchase the 250 W Maxon motor. It operates at 24 V, has a nominal speed of 9090 rev/min, and nominal torque of 0.285 N-m. Using a gearbox ratio of 27:1, the output angular velocity and torque become 35 rad/s and 7.7 N-m respectively. This allows the vehicle to travel at a top speed of 13 mph and up a maximum incline of 7 degrees. It is also able to produce a maximum torque of 113 N-m for very short periods of time (useful for climbing curbs or bumps).

Motor Control and Feedback

Because Maxon does not supply motor controllers capable of taking advantage of the full capacity of the EC 45 250W motors, several other suppliers were contacted. While power handling capacity was the principal metric for choosing a suitable controller, compactness, feedback support, and ease of computer interfacing were also considered. A pair of single channel Roboteq BL1500BP brushless DC motor controllers was chosen for our application.

Although the decision had been made previously to forgo the inclusion of integrated incremental quadrature encoders by the factory in the drive motors, later consultation with a robotics veteran as well as the necessity of feedback for closed loop motor speed control resulted in a reversal of this position. Because retrofitting of the motors would be time consuming and expensive, E6 encoders from US Digital were selected to be fitted to the output shaft of the gearbox. The E6 line was among few that supported such a large shaft diameter, and fit cleanly into our existing design without modification or clearancing. Encoder support was added to the BL1500BP motor controllers through the addition of a Roboteq encoder support add-on board.

Sensor Selection and Design

Because the primary mission of the VT-MAGV vehicle is high precision 3D mapping and point cloud generation, a wide array of sensors were researched and implemented for this task. Following is a review of those systems that we were able to repurpose for competing in IGVC. If our goal had been simply to create a vehicle for the competition, our choices would have been more conservative and less expensive. However, we believe that the increased performance provided by these systems will be an advantage now and in future years.

Machine Vision

To perform color recognition during navigation, we use a machine vision camera. The Basler Scout scA640-70gc is used for this. It is very small, weighing only 150 grams, and can capture VGA-resolution images at a maximum of 71 fps. The camera is shown in Figure 5.

Figure 5. Basler Scout Machine Vision Camera

GNSS + Inertial Navigation System

An important factor in meeting the navigation and localization goals for this project is the inclusion of a suitable inertially-aided GNSS receiver that is compatible with the Trimble BX960 RTK base station that is owned by the Virginia Tech VAL. Because of the excellent performance of the Trimble-based systems that were tested in the past, the Trimble subsidy Applanix was initially contacted for available systems. Unfortunately, the lowest-cost turnkey Trimble/Applanix setup, the POS LV 210, far exceeded the GNSS-compromised performance requirements of the project, and at $42,000 was priced in excess of our budgetary restrictions.

Additional turnkey GNSS+INS systems were evaluated, including the Sepentrio AstRx2i and the Novatel SPAN-CPT. Both were fully capable of high-performance RTK positioning in conjunction with the Trimble base station. While neither unit approached the dead-reckoning performance of the Trimble, which integrated a military-grade IMU, both were considerably more inexpensive. The Sepentrio unit, at $14,000, integrated a lower-quality, off the shelf xSens IMU providing only 0.5 deg of heading and orientation accuracy, while the Novatel SPAN-CPT was capable of an order of magnitude better performance for $23,000, as well as superior sensor fusion algorithms providing a much more robust state solution. The Novatel SPAN-CPT system was selected and delivery was received at the beginning of April.

A custom LabVIEW library was created to interface with the SPAN-CPT, and was successfully tested in both single-point and differential (RTK) solution modes. In our testing, the SPAN-CPT can provide a full position-velocity-attitude solution at 100 Hz with accuracies of ±1cm for position and ±0.01 degree attitude.

Single-Plane LIDAR

To conform to the software architecture we are borrowing from our sister project, obstacle avoidance data will be largely provided by a Hokuyo UTM-30lx single-plane LIDAR. The system is compact, lightweight, performs well outdoors, and we have an extensive amount of experience integrating it with LabVIEW.

Cost Analysis.

After completing the platform mechanical design, price quotes were requested for the different components and materials needed to build the platform. The cost of the platform design consists of materials and mechanical components. The drivetrain of the vehicle which includes the battery and the two motors had the largest impact on the total cost to build the platform. As shown in Table 4, the drive train cost $3578.60.The total cost to build the platform is $5,638.87.

Table 4. Mechanical platform parts and materials total cost.

Item	Part Number	Cost (ea)	Quantity	Totals
1x2 6061 Box Tube 1/8" Wall 6' Long	6546K393	$32.05	3	$96.15
2.25x4 6061 Channel 0.19" Base 0.29" Leg 5' Long	1630T18	$55.38	1	$55.38
2x2 6061 Angle 1/8" Thick 8' Long	8982K25	$32.27	1	$32.27
24x24 6061 Sheet 1/8" Thick	89015K48	$71.56	2	$143.12
Lithium Iron Phosphate Battery	Customized	$2232.00	1	$2232.00
Protection Circuit Board	PCM-LFP25.6V100A	$225.95	1	$225.95
Maxon Motor	EC 45 136210	$673.30	2	$1346.60
Gear Head	GP62 110502	$603.70	2	$1207.40
Machine Shop - Welding		$300.00		$300.00
			Total	**$5,638.87**

For the waypoint navigation and mapping system, we used a Novatel GPS, a Hokuyo raging sensor, and a Scout Camera. The three sensors cost a total of $29,408.10. As shown in Table 5, the total cost for sensors and computers required is $30,700.

Table 5. Sensors and required accessories total cost.

Item	Part Number	Cost(ea)	Quantity	Totals
Scout Machine Camera SCA640	780884-01	$818.09	1	$818.09
Novatel GNS+INS with Antenna	SPAN-CPT	$23000	1	$23000
Hokuyo	UTM-30LX	$5590	1	$5590
Toradex compact computer	Robin Z530 V2.0	$517	1	$517
Roboteq Motor Controller with Encoder support	BL1500 BP	$330	2	$660
US Digital E6 Encoders	E6	$95	2	$190
			Total	**$30,700**

Faculty Design Project Certification

As this project was started from scratch in Fall 2010, all of the deliverable results have been the direct result of the efforts of this year's student team. This statement certifies that the design and engineering process described in this report reflects the significant body of original work that the student team completed over the course of the semester.

____

Advisor Signature